Supplemental Material

Detailed Methods

Generation and characterization of microRNA transgenic mice. miR-143 and miR-378 transgenic mice were created via cloning genomic DNA fragments flanking microRNA stem-loop precursor regions (lengths as shown in **Figure 2a** of the main text) into the SalI/HindIII cloning site of the αMHC/*Myh6* cardiac transgenic promoter construct. Mice were housed according to procedures approved by the Washington University Institutional Animal Care and Use Committee. miR-143 and -378 overexpression in hearts were initially measured using Applied Biosystems TaqMan microRNA qPCR assays with U6 snRNA as reference RNA (data not shown); later microRNA-Seq analysis (see below), as documented in the manuscript, found similar overexpression levels.

Mouse adult cardiomyocyte isolation and gene expression analysis. Cardiomyocyte and nonmyocyte fractions were separately isolated from the hearts of three 8 week-old, wild-type FVB/N mice, as previously described [1]. Following 3 rounds of gravity filtration and washing with ice-cold PBS, myocytes were immediately dissolved in Trizol (Invitrogen) and total RNA was prepared. In order for sufficient nonmyocytes to be available for gene expression assays, cells were plated in tissue culture dishes in DMEM / 10% fetal calf serum / antibiotics, grown at 37 C / 5% CO_2, and passaged once. Cell monolayers were harvested directly into Trizol. Applied Biosystems TaqMan microRNA and mRNA qPCR assays were performed as previously described [2], with the following mRNA expression probes:

Actc1:	Mm01333821_m1
Col1a1:	Mm00801666_g1
Gapdh:	Mm99999915_g1
Myh6:	Mm00440359_m1
Tpm1:	Mm00600378_m1

microRNA-Seq for microRNA expression analysis. Libraries were prepared with TruSeq Small RNA Sample Prep Kits (Illumina) following the manufacturer's protocols, as previously described [2]. Briefly, small RNAs from 1 μg total mouse heart RNA were sequentially ligated with 3′ and 5′ adapters, followed by reverse transcription to produce single stranded cDNAs, which were then amplified by PCR with primers including indexing capabilities to distinguish individual libraries after flowcell processing. The amplified libraries were size-selected/gel-purified and quantified. Twelve libraries were pooled in equimolar amounts and diluted to 14 pmol/L for cluster formation on a single flow cell lane, followed by single-end sequencing (50 nt reads, not including the index determination) on an Illumina HiSeq 2000 sequencer. Alignment and quantitation of microRNA sequencing reads was performed by following the E-miR pipeline as described [3] with minor modifications to the EmiR-Bowtie.pl Perl script to allow the Bowtie aligner [4] to correctly map those microRNAs that arise from multiple genomic loci.

microRNA annotation using miRBase 19. Previous nomenclature for microRNAs often described the minor product (passenger strand) of a microRNA stem-loop structure as a miR* form. In this manuscript, we have annotated mouse microRNAs according to the nomenclature used by miRBase 19, released in August 2012 (http://www.mirbase.org/) [5, 6]. microRNAs are designated as -5p or -3p forms according to their site of origin in the microRNA stem-loop precursor. While information on whether a microRNA form is ‘major’ or ‘minor’ is sometimes available from deep-sequencing data accumulated in the miRBase database from a variety of tissues, we have designated ‘major’ and ‘minor’ forms in mouse hearts according to the deep-sequencing data that we obtained for this paper.

mRNA-Seq for mRNA expression analysis. mRNA-sequencing was performed essentially as described [2, 7-9], using Illumina HiSeq 2000 sequencers and library indexing rather than bar-coding. Using prior criteria that a meaningfully expressed transcript should be present at a level equivalent to at least 1 mRNA copy/cell (3 FPKM; fragment [reads] per kilobase of exon per million mapped reads) [2, 7-9], or as an alternate, that a detectable transcript must map to at least 1 millionth of the total mapped reads in an individual library, we identified approximately 9,500 coding mRNAs in mouse hearts. Concordance of these cardiac transcriptomes with those from previous RNA-Seq studies was high [2, 7-9].

We and others have extensively compared RNA-sequencing analyses to microRNA and mRNA microarrays, finding that RNA-sequencing analyses generally offer superior dynamic range and accuracy (Supporting Information of [2]). In addition, we have validated differential expression results from sequencing analyses with RT-qPCR techniques in several prior studies [2, 7, 10].

Calculation of differential gene expression using the DESeq package. In comparison to previous analyses using Partek Genomics Suite to compare FPKM values of individual mRNAs [1, 6-8], we used DESeq [11] to normalize read depth across multiple sequencing libraries, to calculate fold-changes, and to derive individual pairwise comparison p-values and false discovery rates (FDRs). This statistical approach, using a negative binomial distribution in comparison to the normal (Gaussian) distribution used by Partek on log-transformed data, is designed to be more robust in contexts where relatively few genes are highly abundant and there is a majority of less abundant genes. While DESeq takes the non-normalized, absolute number of aligned reads as input, we have reported microRNA and mRNA abundance in the main text and remainder of the Online Information as Reads per Million aligned to microRNA species (RpM) for microRNAs, and FPKM for mRNAs, although the underlying fold-change and p-value / FDR comparisons used DESeq's internal methods of library normalization. We compared the DESeq method to Partek methods using FPKM and found similar direction and magnitude of changes in individual mRNAs (data not shown). However, DESeq tended to be more conservative in its assignment of p-values and FDRs.

Cardiac microRNAs and mRNAs regulated in microRNA-transgenic mice were defined using a threshold of 25% (increased or decreased) and a FDR of 0.05. Partek Genomics Suite 6.6 (Partek, St. Louis, MO) was used to derive principal components analysis plots, fold-change vs p-value volcano plots, and unsupervised hierarchical clustering heatmaps.

Explanation of principal component analysis plots: (used in **Figures 4a** and **4b** as exploratory data analysis tools). Principal Components Analysis (PCA) is an exploratory multivariate statistical technique for simplifying complex data sets [12-14].The number of principal components is less than or equal to the number of original variables. This transformation is defined in such a way that the first principal component has the largest possible variance (that is, accounts for as much of the variability in the data as possible), and each succeeding component in turn has the highest variance possible under the constraint that it be orthogonal to (i.e., uncorrelated with) the preceding components. Principal components analysis has been used in a wide range of biomedical problems, including the analysis of microarray data in search of outlier genes [15] as well as the analysis of other types of expression [16, 17]. We and others use this data analysis method and graphical presentation for our RNA-sequencing work (see Figure 4 of [7] and the Supplemental Methods of [2]) because it offers a compact way of viewing a great deal of (multidimensional) data in a fairly intuitive fashion. The above description is adapted from [18].

Informatic analyses. To compare the numbers of likely mRNA targets of primarily and secondarily regulated microRNAs (**Figure 6**, main text) we used our previously described FastamiRs algorithm [2] (http://epigenomics.wustl.edu/edwardsLab/index.php/downloads), since it permits prediction of targets for microRNA passenger or minor strands that are not present in the current TargetScan database.

Overexpressed or upregulated microRNAs were used as input to search the set of downregulated mRNAs (defined using the genome-wide significance criteria above); separate processing was carried out for miR-378 and miR-499 TG mice. Putative target mRNAs were stringently defined as those with a perfect match to the microRNA nucleotide 2-7 'seed' region (G:U base pairing was excluded from consideration on the basis of recent work demonstrating that G:U pairing is poorly tolerated in the seed region for fly Ago2 [19]), a stretch of at least 7 contiguously paired nucleotides (which may include the 'seed'), and with miR binding in the 3'UTR rather than in coding sequences or the 5'UTR.

miR-378- and miR-499-regulated transcription factor binding analysis for promoter regions of regulated miRs, Figure 7: we first used the RIKEN transcription factor database (http://genome.gsc.riken.jp/TFdb, accessed 11/5/12) to identify 1678 transcription factors or accessory proteins, and found 869 of these to be expressed in hearts (using the same abundance criteria we used in our other RNA-seq data throughout the paper). We then obtained predictions for miR-378 or miR-499 binding from the latest version of TargetScan (v6.2), resulting in 15 and 21 potentially microRNA-regulated entities, respectively (**Online Table IV**). Finally, the transcription factor-binding prediction database MAPPER [20] (http://bio.chip.org/mapper) was used to identify putative binding sites 10 kb upstream of the start of the pre-miR, or for those cases in which the pre-miR was present in the intron of a host gene, 10 kb upstream of the transcription start site (**Online Table V**).

'Defined miR-378 targets' in **Figure 7** (light red box) are derived from **Online Table III**, and are those mRNAs predicted by FastamiRs to be downregulated by miR-378-3p and by no other upregulated microRNA. 'Indirect miR-378 targets' in **Figure 7** are those mRNAs which were upregulated in miR-378 transgenic hearts (**Online Table I**). miR-99a targets were those mRNAs predicted by TargetScan v6.2, and known to be expressed in the heart from our deep sequencing data. The categories of 'muscle growth and development', 'muscle contraction' and 'metabolism' were obtained from MetaCore (http://thomsonreuters.com/products_services/science/systems-biology/) / GeneOntology analysis of the defined and indirect miR-378 target gene lists, and the miR-99a TargetScan gene list.

Online Figures and Figure Legends

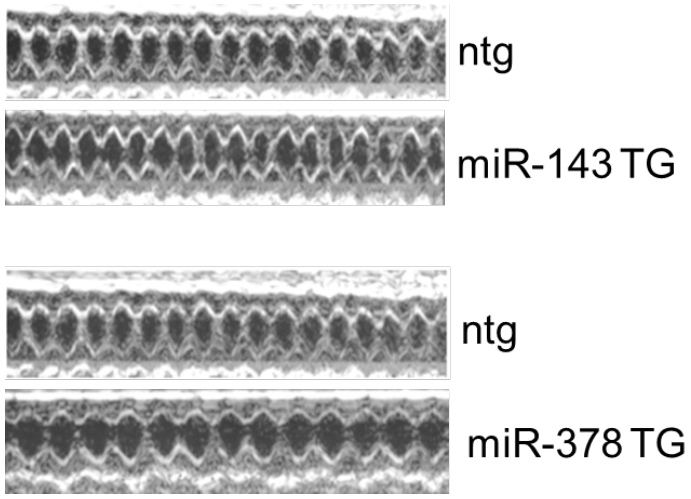

Online Figure I. *Echocardiographic examination of miR-143 and miR-378 transgenic hearts at 8 weeks of age, relative to littermate controls.* Representative M-mode echocardiograms on microRNA transgenic hearts and age- and sex-matched littermate controls.

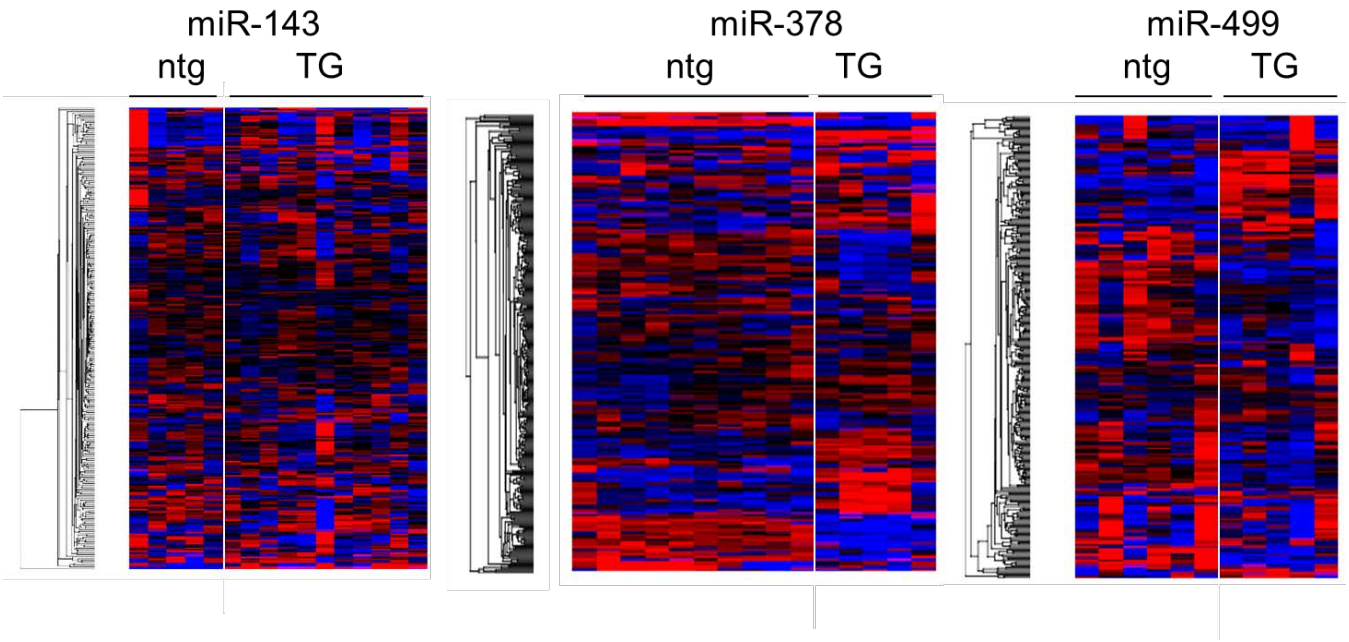

Online Figure II. *Transcriptome-wide microRNA effects of miR-143, -378, and -499.* Unsupervised hierarchical clustering of expression levels for the 300 cardiomiRs in miR-143, -378 and -499 transgenic hearts, compared to littermate controls. Blue indicates downregulation while red indicates upregulation relative to mean level for each microRNA.

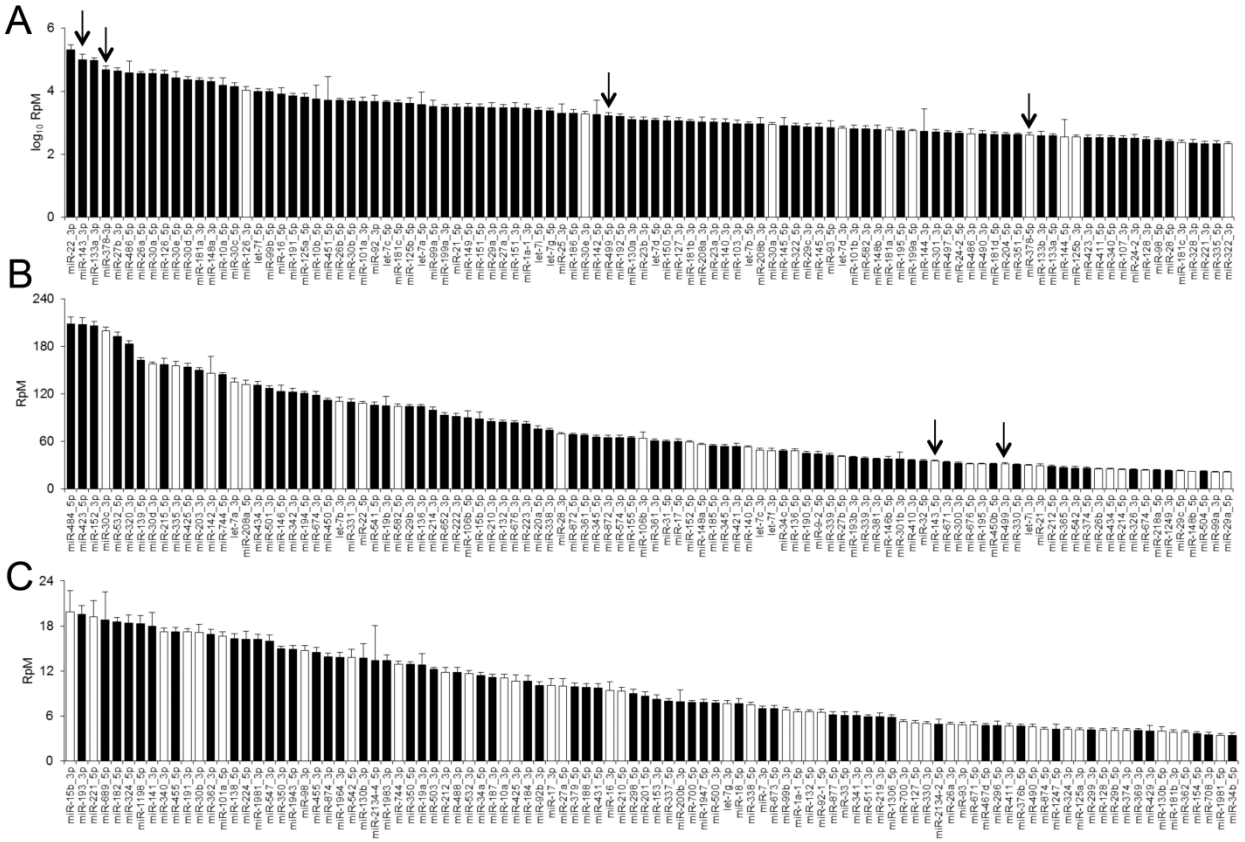

Online Figure III. *microRNA deep sequencing in nontransgenic mouse hearts.* Contextual abundance of cardiomiR guide (black) and passenger (white) strands in 8 wk mouse hearts. **A,** most abundant 100 cardiomiRs (log_{10} scale); **B** and **C** are second and third tiers of 100 cardiomiRs (linear scales). Arrows indicate positions of guide and passenger strands for miR-143 -378, and -499.

Supplemental Tables

Online Table I is supplied as an Excel workbook (.xls)

Online Table I. *mRNAs regulated in miR-143, -378 and -499 transgenic hearts.* Regulated mRNAs were defined as those changed by at least 25% at FDR < 0.05, compared to littermate nontransgenics. The mean FPKM (abundance) of each mRNA in nontransgenic hearts is shown, together with fold-change and FDR in transgenic hearts calculated by DESeq. mRNAs are sorted in order of fold-change, from the most downregulated to the most upregulated. Separate Excel tabs are provided for each of the miR-143, -378 and -499 transgenic heart comparisons.

Online Table II is supplied as an Excel workbook (.xls)

Online Table II. *Regulation amongst 300 cardiomiRs in miR-143, -378 and -499 transgenic hearts.* Similarly to the mRNA analysis in Online Table I, regulated microRNAs were defined as those changed by at least 25% at FDR < 0.05, compared to littermate nontransgenics. MicroRNA expression is given as DESeq-adjusted 'baseMeans', representing the number of sequencing reads obtained for each microRNA, adjusted for sequencing depth (see **Detailed Methods**). Aligned read counts for microRNA libraries averaged 7.1×10^6; thus, any microRNA with less than 7 reads (~1 millionth of the total) was eliminated from further analysis. MicroRNAs are sorted in order of fold-change, from the most downregulated to the most upregulated. Separate Excel tabs are provided for each of the miR-143, -378 and -499 transgenic heart comparisons.

Online Table III is supplied as an Excel workbook (.xls)

Online Table III. *Downregulated mRNAs in miR-378 and -499 transgenic hearts, predicted to be targets of primarily and secondarily upregulated microRNAs.* The FastamiRs algorithm [2] was used with stringent parameters (see **Detailed Methods**) to predict targeting of downregulated mRNAs by upregulated microRNAs.

Online Table IV

miR	Gene ID	Gene symbol	Gene name
378	ENSMUSG00000018983	E2f2	E2F transcription factor 2
378	ENSMUSG00000028266	Lmo4	LIM domain only 4
378	ENSMUSG00000051510	Mafg	v-maf musculoaponeurotic fibrosarcoma oncogene family, protein G (avian)
378	ENSMUSG00000063358	Mapk1	mitogen activated protein kinase 1
378	ENSMUSG00000000282	Mnt	max binding protein
378	ENSMUSG00000028890	Mtf1	metal response element binding transcription factor 1
378	ENSMUSG00000028423	Nfx1	nuclear transcription factor, X-box binding 1
378	ENSMUSG00000021111	Papola	poly (A) polymerase alpha
378	ENSMUSG00000051413	Plagl2	pleiomorphic adenoma gene-like 2
378	ENSMUSG00000049647	Purb	purine rich element binding protein B
378	ENSMUSG00000006456	Rbm14	RNA binding motif protein 14
378	ENSMUSG00000032238	Rora	RAR-related orphan receptor alpha
378	ENSMUSG00000022623	Shank3	SH3/ankyrin domain gene 3
378	ENSMUSG00000051910	Sox6	SRY-box containing gene 6
378	ENSMUSG00000015837	Sqstm1	sequestosome 1
499	ENSMUSG00000030232	Aebp2	AE binding protein 2
499	ENSMUSG00000019947	Arid5b	AT rich interactive domain 5B (Mrf1 like)
499	ENSMUSG00000057098	Ebf1	early B-cell factor 1
499	ENSMUSG00000032035	Ets1	E26 avian leukemia oncogene 1, 5' domain
499	ENSMUSG00000029563	Foxp2	forkhead box P2
499	ENSMUSG00000021944	Gata4	GATA binding protein 4
499	ENSMUSG00000050240	Hic2	hypermethylated in cancer 2
499	ENSMUSG00000032178	Ilf3	interleukin enhancer binding factor 3
499	ENSMUSG00000021690	Jmy	junction-mediating and regulatory protein
499	ENSMUSG00000020160	Meis1	myeloid ecotropic viral integration site 1
499	ENSMUSG00000028647	Mycbp	c-myc binding protein
499	ENSMUSG00000027201	Myef2	myelin basic protein expression factor 2, repressor
499	ENSMUSG00000048490	Nrip1	nuclear receptor interacting protein 1
499	ENSMUSG00000021816	Ppp3cb	protein phosphatase 3, catalytic subunit, beta isoform
499	ENSMUSG00000004771	Rab11a	RAB11a, member RAS oncogene family
499	ENSMUSG00000023927	Satb1	special AT-rich sequence binding protein 1
499	ENSMUSG00000041540	Sox5	SRY-box containing gene 5
499	ENSMUSG00000051910	Sox6	SRY-box containing gene 6
499	ENSMUSG00000063060	Sox7	SRY-box containing gene 7
499	ENSMUSG00000032228	Tcf12	transcription factor 12
499	ENSMUSG00000039473	Ubn1	ubinuclein 1

Online Table IV. *Cardiac-expressed transcription factors predicted to be regulated by miR-378-3p or miR-499-5p according to TargetScan v6.2.* Transcription factor genes were obtained from the RIKEN transcription factor database, selected for cardiac expression, and filtered for TargetScan-predicted regulation by miRs-378 or -499 (see **Detailed Methods**).

Online Table V is supplied as an Excel workbook (.xls)

Online Table V: *Putative transcription factor binding sites in microRNA promoter regions.* Hits predicted by MAPPER [20] in microRNA promoter regions (see **Detailed Methods**).

Supplemental References

1. Dorn GW, 2nd, Robbins J, Ball N, Walsh RA. Myosin heavy chain regulation and myocyte contractile depression after LV hypertrophy in aortic-banded mice. *Am J Physiol.* 1994;267:H400-405.
2. Hu Y, Matkovich SJ, Hecker PA, Zhang Y, Dorn GW, II. Epitranscriptional orchestration of genetic reprogramming is an emergent property of stress-regulated cardiac microRNAs. *Proc Natl Acad Sci USA.* 2012;109:19864-19869.
3. Buermans HP, Ariyurek Y, van Ommen G, den Dunnen JT, t Hoen PA. New methods for next generation sequencing based microRNA expression profiling. *BMC Genomics.* 2010;11:716.
4. Langmead B, Trapnell C, Pop M, Salzberg SL. Ultrafast and memory-efficient alignment of short DNA sequences to the human genome. *Genome Biol.* 2009;10:R25.
5. Griffiths-Jones S, Grocock RJ, van Dongen S, Bateman A, Enright AJ. miRBase: microRNA sequences, targets and gene nomenclature. *Nucleic Acids Res.* 2006;34:D140-144.
6. Kozomara A, Griffiths-Jones S. miRBase: integrating microRNA annotation and deep-sequencing data. *Nucleic Acids Res.* 2011;39:D152-157.
7. Matkovich SJ, Hu Y, Eschenbacher WH, Dorn LE, Dorn GW, II. Direct and indirect involvement of microRNA-499 in clinical and experimental cardiomyopathy. *Circ Res.* 2012;111:521-531.
8. Dorn GW, 2nd, Matkovich SJ, Eschenbacher WH, Zhang Y. A human 3' miR-499 mutation alters cardiac mRNA targeting and function. *Circ Res.* 2012;110:958-967.
9. Matkovich SJ, Van Booven DJ, Eschenbacher WH, Dorn GW, 2nd. RISC RNA sequencing for context-specific identification of in vivo microRNA targets. *Circ Res.* 2011;108:18-26.
10. Matkovich SJ, Zhang Y, Van Booven D, Dorn GW, 2nd. Deep mRNA sequencing for in vivo functional analysis of cardiac transcriptional regulators. Application to Gaq. *Circ Res.* 2010;106:1459-1467.
11. Anders S, Huber W. Differential expression analysis for sequence count data. *Genome Biol.* 2010;11:R106.
12. Pearson K. On lines and planes of closest fit to systems of points in space. *Philosophical Magazine* 1901;2:559-572.
13. Basilevsky A. *Statistical Factor Analysis and Related Methods, Theory and Applications*: John Wiley & Sons; New York, NY; 1994.
14. Everitt BS, Dunn G. *Applied Multivariate Data Analysis*: Oxford University Press; New York, NY; 1992.
15. Hilsenbeck SG, Friedrichs WE, Schiff R, O'Connell P, Hansen RK, Osborne CK, Fuqua SA. Statistical analysis of array expression data as applied to the problem of tamoxifen resistance. *J Natl Cancer Inst.* 1999;91:453-459.
16. Vohradsky J, Li XM, Thompson CJ. Identification of procaryotic developmental stages by statistical analyses of two-dimensional gel patterns. *Electrophoresis.* 1997;18:1418-1428.
17. Craig JC, Eberwine JH, Calvin JA, Wlodarczyk B, Bennett GD, Finnell RH. Developmental expression of morphoregulatory genes in the mouse embryo: an analytical approach using a novel technology. *Biochem Mol Med.* 1997;60:81-91.
18. Raychaudhuri S, Stuart JM, Altman RB. Principal components analysis to summarize microarray experiments: application to sporulation time series. *Pac Symp Biocomput.* 2000:455-466.
19. Wee LM, Flores-Jasso CF, Salomon WE, Zamore PD. Argonaute divides its RNA guide into domains with distinct functions and RNA-binding properties. *Cell.* 2012;151:1055-1067.
20. Marinescu VD, Kohane IS, Riva A. The MAPPER database: a multi-genome catalog of putative transcription factor binding sites. *Nucleic Acids Res.* 2005;33:D91-97.